Journal of Medical Systems (2019) 43: 99
https://doi.org/10.1007/s10916-019-1203-y

IMAGE & SIGNAL PROCESSING

Computer-Aided Diagnosis System for Detection of Stomach Cancer with Image Processing Techniques

Ali Yasar[1] · Ismail Saritas[2] · Huseyin Korkmaz[3]

Received: 27 December 2018 / Accepted: 11 February 2019 / Published online: 14 March 2019

Abstract

Stomach cancer is a type of cancer that is hard to detect at an early stage because it gives almost no symptoms at the beginning. Stomach cancer is an increasing incidence of cancer both in the World as well as in Turkey. The most common method used worldwide for gastric cancer diagnosis is endoscopy. However, definitive diagnosis is made with endoscopic biopsy results. Diagnosis with endoscopy is a very specific and sensitive method. With high-resolution endoscopy it is possible to detect mild discolorations, bulges and structural changes of the surface of the mucosa. However, because the procedures are performed with the eye of a doctor, it is possible that the cancerous areas may be missed and / or incompletely detected. Because of the fact that the cancerous area cannot be completely detected may cause the problem of cancer recurrence after a certain period of surgical intervention. In order to overcome this problem, a computerized decision support system (CDS) has been implemented with the help of specialist physicians and image processing techniques. The performed CDS system works as an assistant to doctors of gastroenterology, helping to identify the cancerous area in the endoscopic images of the scaffold, to take biopsies from these areas and to make a better diagnosis. We believe that gastric cancer will be helpful in determining the area and biopsy samples taken from the patient will be useful in determining the area. It is therefore considered a useful model.

Keywords Stomach cancer · Region growing · Statistical region merging · Statistical region merging with region growing · Segmentation · Image processing · Computerized decision support(CDS) system

Introduction

Cancer is the most important problem for human life [1]. In addition to the high mortality rate, early detection and diagnosis are become crucial to understand cancer, but depending on the type of cancer, diagnostic procedures can be quite costly [2]. According to statistics from the Ministry of Health, stomach cancer is the second most common type of cancer in our country [3]. Despite a major decline in incidence and mortality over several decades, stomach cancer is still the fourth most common cancer and the second most common cause of cancer death in the World [4]. Stomach cancer is characterized by inhabiting any part of the stomach and generally expanding organs as lymph glands, liver and lungs. Cancer occurs as a result of the development of malign tumors in stomach mucosa for various reasons. Cancer, which is among the most common types of cancer in our country, leads 800,000 people to die in the world annually [5]. Early diagnosis is of great importance in cancer for the treatment to be successful. For this reason, it is important for specialist doctors to monitor the people who have trouble with their stomach with the help of endoscopy at an early phase. While performing endoscopy, your doctor can observe your digestive tract, your stomach and the first parts of your small intestine with the help of a camera with a light. If there are parts that appear to be abnormal, a biopsy is taken for an exact diagnosis. It's possible to catch the disease at an early phase by using endoscopy properly.

This article is part of the Topical Collection on *Image & Signal Processing*

✉ Ali Yasar
aliyasar@selcuk.edu.tr

[1] Computer Programming, Guneysinir Vocational School of Higher Education Selcuk University, Guneysinir, 42190 Konya, Turkey

[2] Faculty of Technology, Electrical and Electronics Engineering Selcuk University, 42031 Konya, Turkey

[3] Department of Gastroenterology, Faculty of Medicine, Selcuk University, 42031 Konya, Turkey

Recently, Computer-aided diagnosis (CAD) systems have been very common and generally, image processing methods and some different techniques are used in these systems [6, 7]. CAD systems have started to become common in recent years in order to diagnose and phase several types of cancer such as lung, brain and breast cancer in parallel with the developments of medical imaging and computer technologies [8]. In our study, computer-aided diagnosis system is recommended for detection and diagnosis of stomach cancer using endoscopy images.

Image processing technique involves studying the images transferred from cameras scanners and similar devices to the computer with the help of special programs. Such image processing is employed in a number of fields such as industry, security, geology, medicine and agriculture. It is used in agriculture to analyze colors in fruit, to classify them, to monitor their development, to measure the size of leaves and to detect weeds [9–13]. In today's medicine, there are many systems for recognizing cancerous cells [14]. Some of these systems are quite expensive systems and their usage is complicated [15]. Indeed, in engineering, there are many image processing methods such as pattern recognition, classification etc. [16]. CDS methods are important for these conditions [17].

1- Increasing the sensitivity for detection of cancer,
2- Reducing the variation in image interpretation and reducing the estimated time,
3- Identification of potential cancer area

In this study, a CDS system, which could detect the area of the stomach that could be cancerous, is recommended by utilizing the endoscopy images of the patients who visited gastroenterology unit of the Selcuk University Medical Faculty. The system consists of two basic sections, which are segmentation and comparison with Ground Truth. At the segmentation stage, cancerous areas were identified, based on RG, SRM and SRMWRG segmentation process; the accuracy rates are compared with those of the area which a specialist doctor designated as a cancerous area. Besides, a complete CDS system was recommended by designing interface software.

Material and method

Of the patients who visited the gastroenterology Department of the Selcuk University Medical Faculty Hospital for 1 year starting from June 2016, those who received stomach cancer diagnosis and from whom biopsy results were taken were included in our study. Images of the patients were taken with Olympus Q260 endoscopy device. These images were studied by a doctor, and the processing work was started. Ground Truth pictures of the area designated by the specialist doctor as cancerous were taken. The segmentation was initiated on the pictures. The general architectural structure of the CDS system designated is seen in Fig. 1. In Fig. 2. the user interface software of the recommended CDS system is seen.

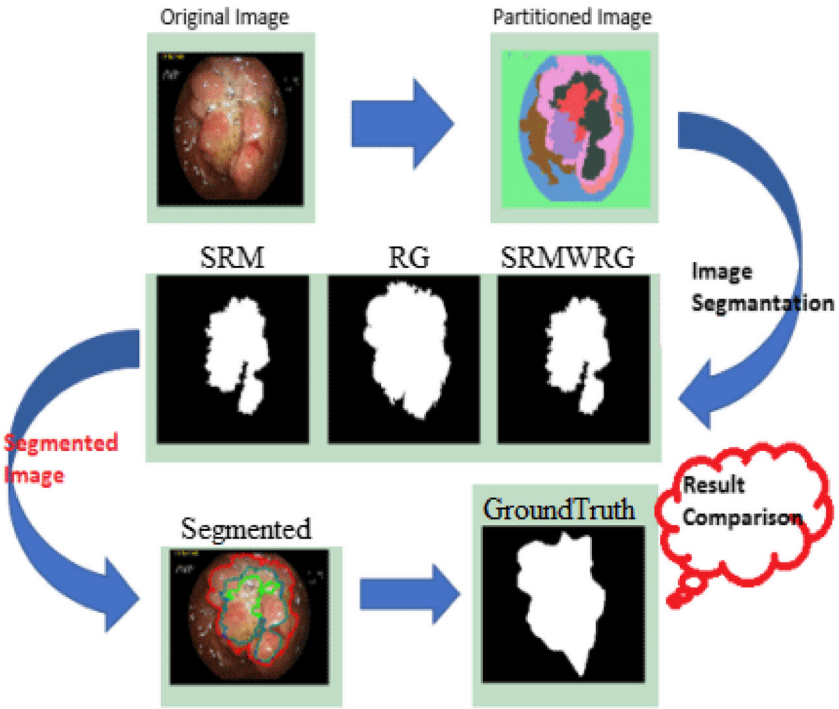

Fig. 1 The architecture of the designed CAD system

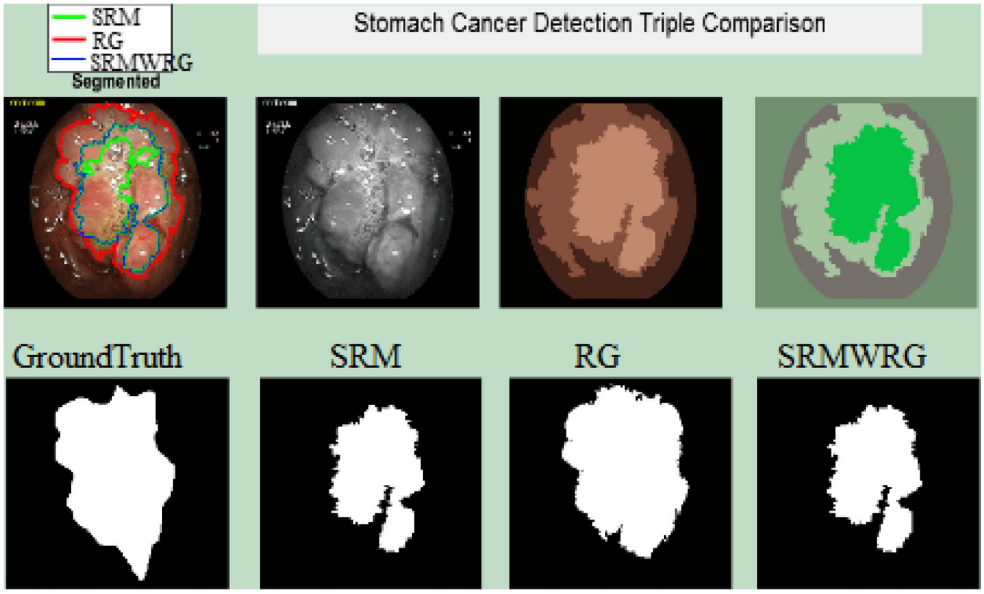

Fig. 2 The interface software of the designed CAD system

Segmentation

The most important stage of image processing and of our study is the segmentation stage. The process of segmentation must be successful for the cancerous area to be diagnosed successfully on an endoscopy image. Three different techniques, RG, SRM and SRMWRG, are used to conduct segmentation in the designed interface, and a comparison of their success was made.

Region growing (RG)

The geometric properties of the regions depend on the area. They are generally considered to be related to two-dimensional areas. The regions may be disconnected, not simply connected, should have smooth boundaries, etc., depending on the region's breeding technique and job objectives [18]. Ultimately, dividing the entire image into half-halves is often the partitioning target. That is, regions are two-dimensional overlaps and no pixel belongs to more than one region. But there is not a single definition that can be allowed to overlap the entire image. The whole image may or may not split. Our discussion of the breeders of the region will begin with the simplest species and become more complex. Most prominent zone producers only aggregate properties of local pixel groups to determine zones [19].

The algorithm of region growing is one of the segmentation techniques favored in image processing applications. Region growing technique is a section- based technique. First, an initial seed is determined. Statistical calculations are conducted between this initial seed and the adjacent points. During the calculation, search parameters as mean intensity value, color and variance are identified. Based on these values, similar regions are clustered and segmentation is conducted. In general, the initial seed is chosen by the user, and segmentation process is initiated on this point. The process is conducted are should be corrected as follows: first, we have to choose a seed pixel as a starting point for each of the required segmentation processes. In the second stage, we combine the same or similar features of the pixel and the areas that have similar features around the seat pixel area on the seed area. Every new pixel is studied until there are no more pixels satisfying requirements [20].

We have to take into account three practical basic problems in applying this method [21].

I. Was a seed pixel that could properly represent the required area chosen or identified?
II. Does the formula contain the adjacent pixels for growth to occur?
III. The rules and or requirements that would complete the process of growing set?

Different areas of an image are joined to a single area with several similarity criteria. Region growing technique is simple, and it can correctly separate the image pixels that have similar features in order to form large areas or objects [22]. RG segmentation scheme can be defined in the region with several features [23]:

$$\bigcup_{i=1}^{n} Ri = R, \tag{1}$$

where R_i is the i^{th} region in an image R, and the image is divided into n regions

$$Ri \cap Rj = \phi, \tag{2}$$

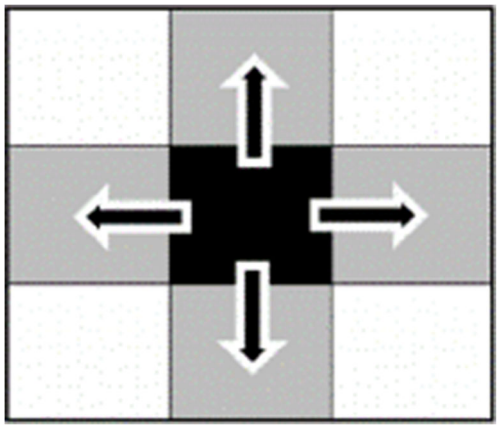

Fig. 3 Seed Point

i.e., two regions i and j are disjoint.

$$P(R_i \cup R_j) = FALSE \quad (3)$$

Which signifies that any logical predicate P defined over two adjacent regions are false; i.e., two regions are different. Similarly, it is required that the region Ri should be a connected region. It is noted in the literature that the region growing approach has two major drawbacks: it requires the selection of appropriate seed points, and a minor intensity variation gives over-segmentation. It may also be noted that, here we have proposed a novel boundary preserving region growing technique so as to remove the aforementioned disadvantages [22].

The process following the stage starts to check the degree of similarity between four neighboring pixel points coming from the point selected as shown in Fig. 3. with the point chosen. We put the tag of the point of choice on a neighboring pixel if it meets the pixel connection criterion. We put the tag of the point of choice on a neighboring pixel if it meets the pixel connection criterion. Giving a higher threshold to check the connection because of the no visibility and love noise in medical images causes a larger area probably covering the whole image to be chosen. In order to prevent this, the process should be terminated if the calculated variance value is below the predetermined threshold value. The implemented state of the Region Growing segmentation process with the help of CAD program is shown in Fig. 4.

Statistical region merging (SRM)

Statistical region merging (SRM) is a novel, colored image segmentation technique for region growing and merging. This method models segmentation as a deduction problem in which statistical areas are observed as a sample of an unknown image which would be formed anew. Among the advantages of this method are its simplicity, its efficiency in calculation and quantification or its excellent performance without using color space transformations [24].

The two key steps of the algorithm are as follows [25].

1) Identify a sort function. The adjacent regions are sorted out depending on to the size of the function.
2) Identify a merging predicate. The merging predicate determines whether the adjacent regions are merged or not.

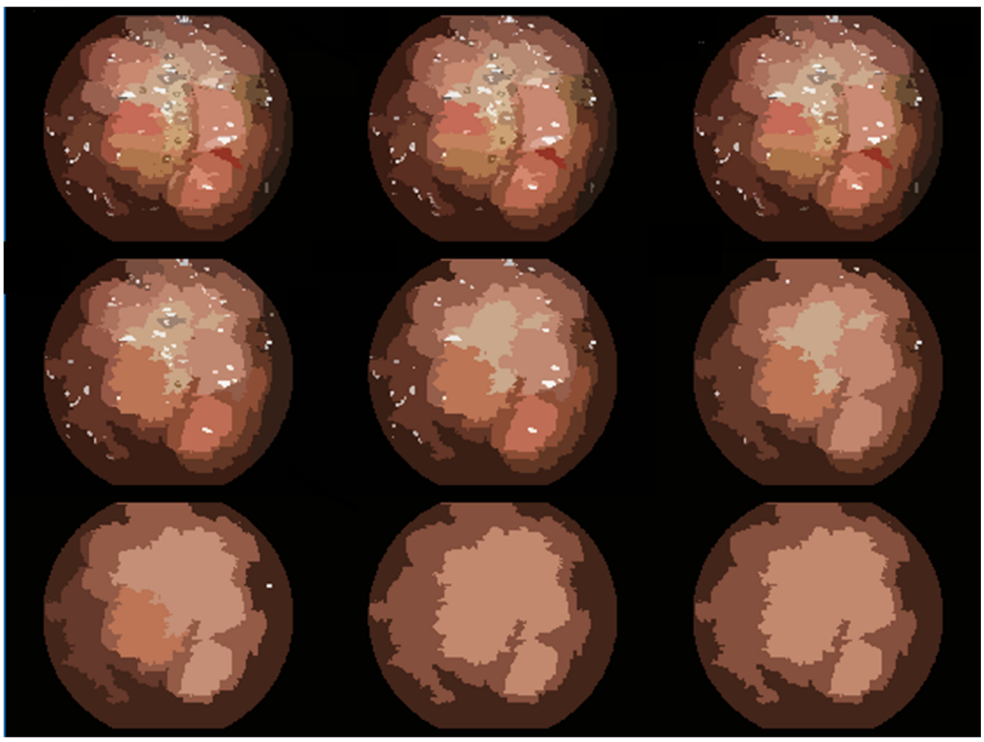

Fig. 4 Region- Growing Segmentation Steps in CAD

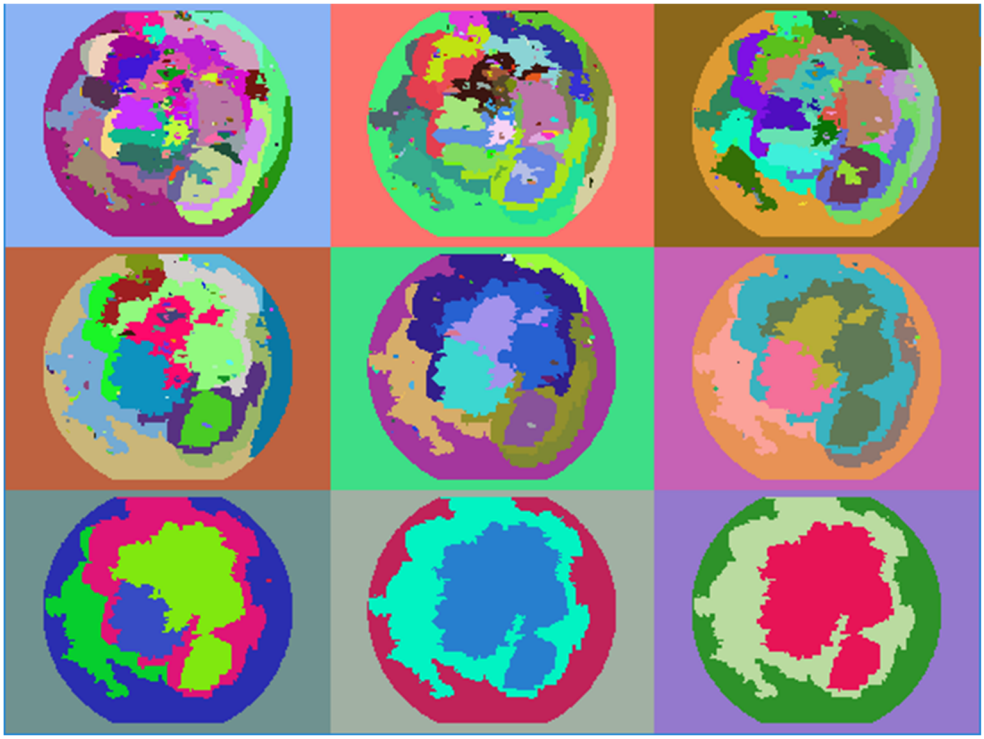

Fig. 5 Statistical Region Merging Segmentation Steps in CAD

It is clear that a sort function and a merging predicate are the bases of the algorithm and they are interactive with each other.

Nielsen and Nock take into consideration a sort function f defined as follows:

$$f\left(p,p^{'}\right) = max_{a\in\{R,G,B\}}\ |P_a^{'}-P_a| \tag{4}$$

Where, $P_a^{'}$, P_a stand for pixel values of a pair of adjacent pixels of the channel a . The following merging predicate is obtained from the Nielsen and Nock model:

$$\mathrm{P(R,R')} = \begin{cases} True. & if\ \forall a\in\{R,G,B\}, \left|\bar{R}'a-\bar{R}\,a\right| \le \sqrt{b^2(R)+b^2(R')} \\ False. & Othewise \end{cases} \tag{5}$$

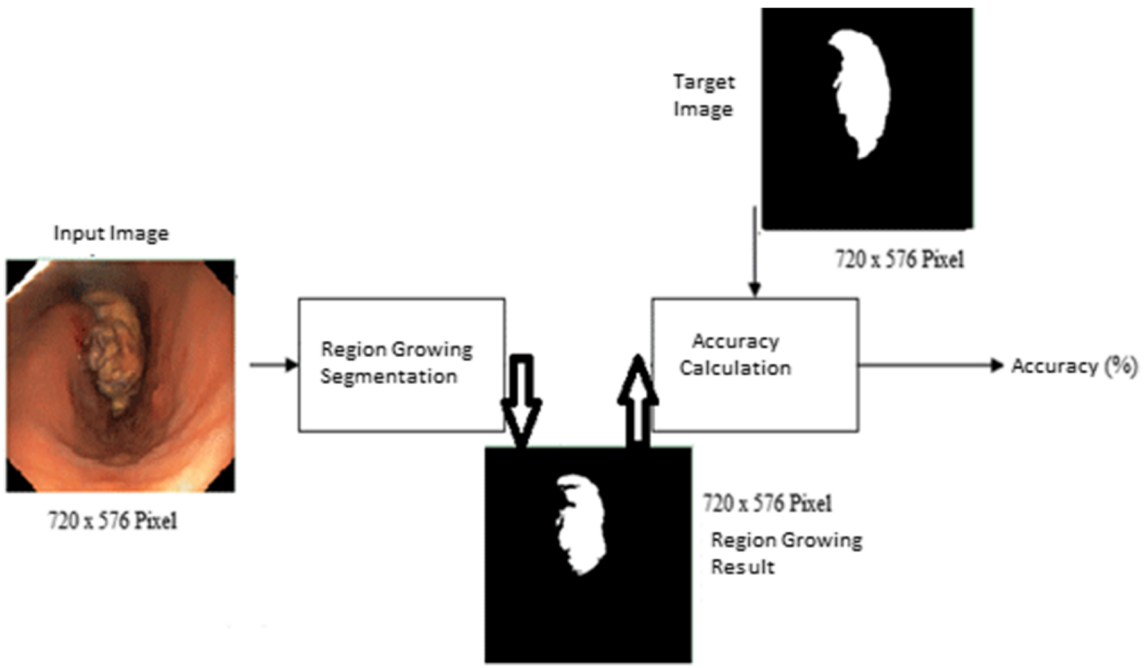

Fig. 6 Block schedules of the RG algorithm

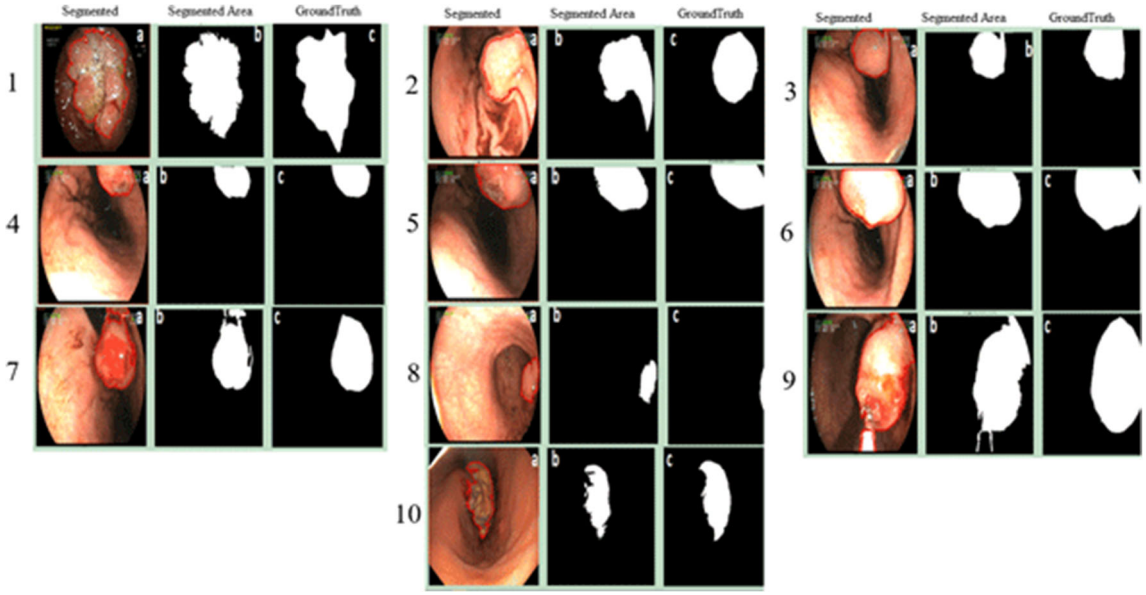

Fig. 7 Original Image, RG Segmented, Gound Truth Images

Where, $b(R) = g\sqrt{\frac{1}{2Q|R|}\left(\ln\frac{|R_{|R|}|}{\delta}\right)}$, $\overline{R}a$ denotes the observed mean value for channel a in region R, and $R_{|R|}$ stands for the set of regions with R pixels. For recognition, more sorting functions and combining predictions can be used to increase the speed and quality of the segmentation. Finally, the SRM algorithm can capture basic structural components of images using simple but effective statistical analysis and has the ability to cope with significant noise, block through clustering and multi-scale segmentation. The implemented state of the Statistical Region Merging segmentation process with the help of CAD program is shown in Fig. 5.

Statistical region merging with region growing (SRMWRG)

First, region merging is conducted on the picture with SRM in the area ticked with this hybrid segmentation method. Then, region growing is conducted on the identified area with RG. In this way, if there is any missing area with SRM, it can be possible to enlarge areas with RG. The steps 2.1.1 and 2.1.2 should be followed one after another on the point.

Experimental studies

The application of RG, SRM and SRMWRG methods

The algorithm is implemented in MATLAB and is run on Intel(R)_Core(TM)_i7-3630QM_CPU_@_2.40GHz PC with 8 GB RAM and Windows10 operating system. The Matlab program was only used for interface and coding. The interface design and the written codes are

Table 1 TP, TN, FP, FN, Accuracy, Sensitivity, Specificity, Precision, ROC and F-Score Values

Application of Image Number	TN	TP	FP	FN	Accuracy	Sensitivity	Specificity	Precision	ROC Curve	F-Score
Image-1	263,584	117,076	20,391	13,669	91,79	89,55	92,82	85,17	91,18	87,30
Image-2	316,495	54,293	32,248	11,684	89,41	82,29	90,75	62,74	86,52	71,20
Image-3	367,567	38,845	60	8248	98,00	82,49	99,98	99,85	91,23	90,34
Image-4	387,248	26,203	159	1110	99,69	95,94	99,96	99,40	97,95	97,64
Image-5	360,125	47,749	58	6788	98,35	87,55	99,98	99,88	93,77	93,31
Image-6	330,045	78,011	6	6658	98,39	92,14	100,00	99,99	96,07	95,90
Image-7	346,227	55,380	4407	8706	96,84	86,42	98,74	92,63	92,58	89,41
Image-8	393,210	14,095	0	7415	98,21	65,53	100,00	100,00	82,76	79,17
Image-9	275,157	116,666	14,052	8845	94,48	92,95	95,14	89,25	94,05	91,06
Image-10	371,572	35,296	740	7112	98,11	83,23	99,80	97,95	91,52	89,99
				Average (%)	96,33	85,81	97,72	92,68	91,76	88,53

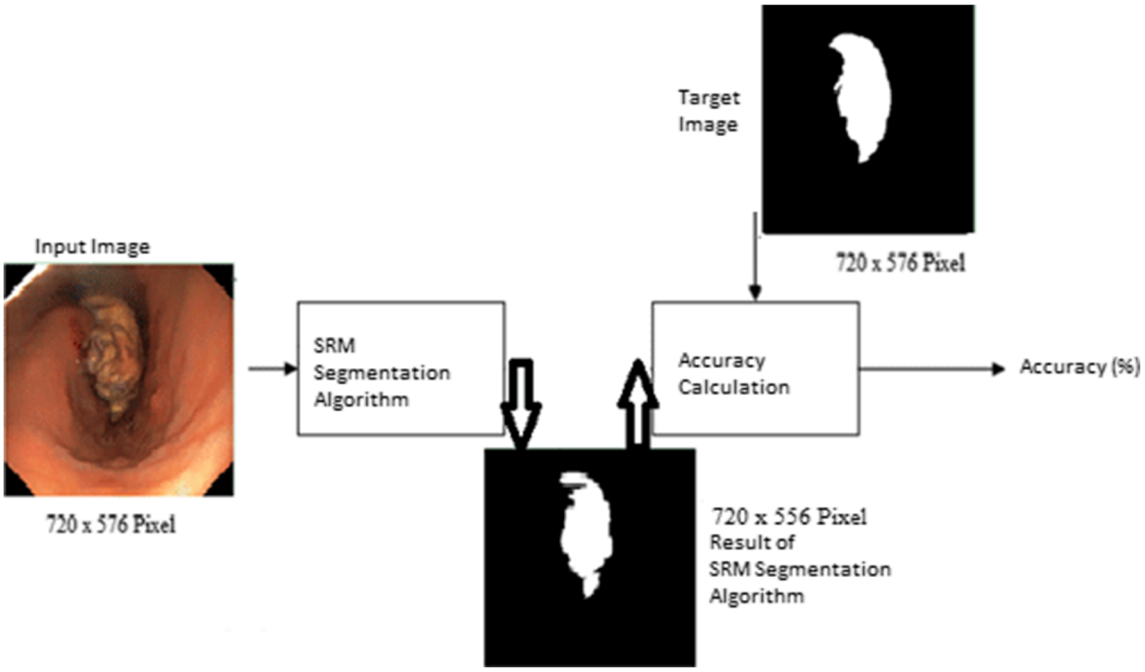

Fig. 8 Block schedules of the SRM algorithm

all done by ourselves. Specialist doctors identified cancerous areas on the pictures obtained from the endoscopic images belonging to different patients in the gastroenterology Department of the Medical Faculty in Selcuk University. Ground Truth pictures of each area were formed. Endoscopy images of nine patients were studied in a semi-automatic way with RG, SRM and SRMWRG segmentation methods using the interface of the CDS system.

Computer decision support for RG

Computer decision support systems are computer applications designed to aid clinicians in making diagnostic and therapeutic decisions in patient care [26]. Figure 6 shows the block diagram of the decision support system of the RG method.

Figure 7 shows the results of the segmentation obtained as a result of the application of the RG algorithm.

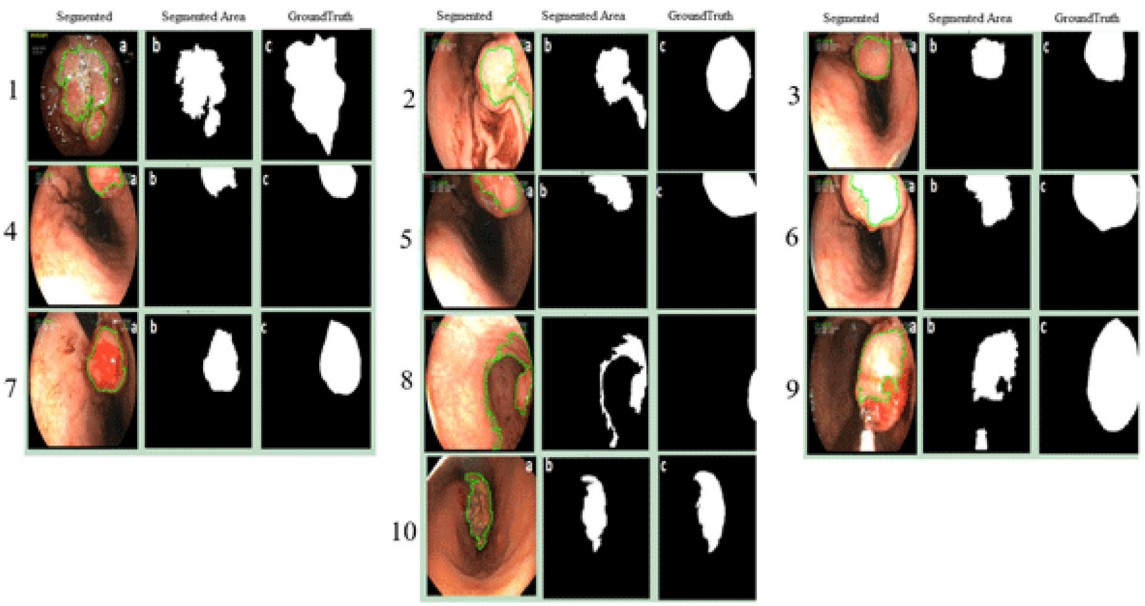

Fig. 9 Original Image, SRM Segmented, Ground Truth Images

Table 2 TP, TN, FP, FN, Accuracy, Sensitivity, Specificity, Precision, ROC and F-Score Values

Application of Image Number	TN	TP	FP	FN	Accuracy	Sensitivity	Specificity	Precision	ROC Curve	F-Score
Image-1	282,107	83,736	1868	47,009	88,21	64,05	99,34	97,82	81,69	77,41
Image-2	337,038	41,117	11,705	24,860	91,18	62,32	96,64	77,84	79,48	69,22
Image-3	367,626	31,679	1	15,414	96,28	67,27	100,00	100,00	83,63	80,43
Image-4	387,316	20,495	91	6818	98,33	75,04	99,98	99,56	87,51	85,58
Image-5	360,183	29,359	0	25,178	93,93	53,83	100,00	100,00	76,92	69,99
Image-6	330,051	47,400	0	37,269	91,01	55,98	100,00	100,00	77,99	71,78
Image-7	350,634	47,420	0	16,666	95,98	73,99	100,00	100,00	87,00	85,05
Image-8	365,951	14,432	27,259	7078	91,72	67,09	93,07	34,62	80,08	45,67
Image-9	282,815	64,225	6394	61,286	83,68	51,17	97,79	90,95	74,48	65,49
Image-10	372,308	34,620	4	7788	98,12	81,63	100	99,99	90,82	89,89
				Average (%)	92,85	65,24	98,68	90,08	81,96	74,05

Table 1 shows the accuracy, sensitivity, specificity, ROC curve performance results and the average values of these results.

Table 2 shows the accuracy, sensitivity, specificity, ROC curve performance results and the average values of these SRM segmented results.

Computer decision support for SRM

Figure 8 shows the block diagram of the decision support system of the SRM method.

Figure 9 shows the results of the segmentation obtained as a result of the application of the SRM algorithm.

Computer decision support for SRMWRG

Figure 10 shows the block diagram of the decision support system of the SRMWRG method.

Figure 11 shows the results of the segmentation obtained as a result of the application of the SRMWRG algorithm.

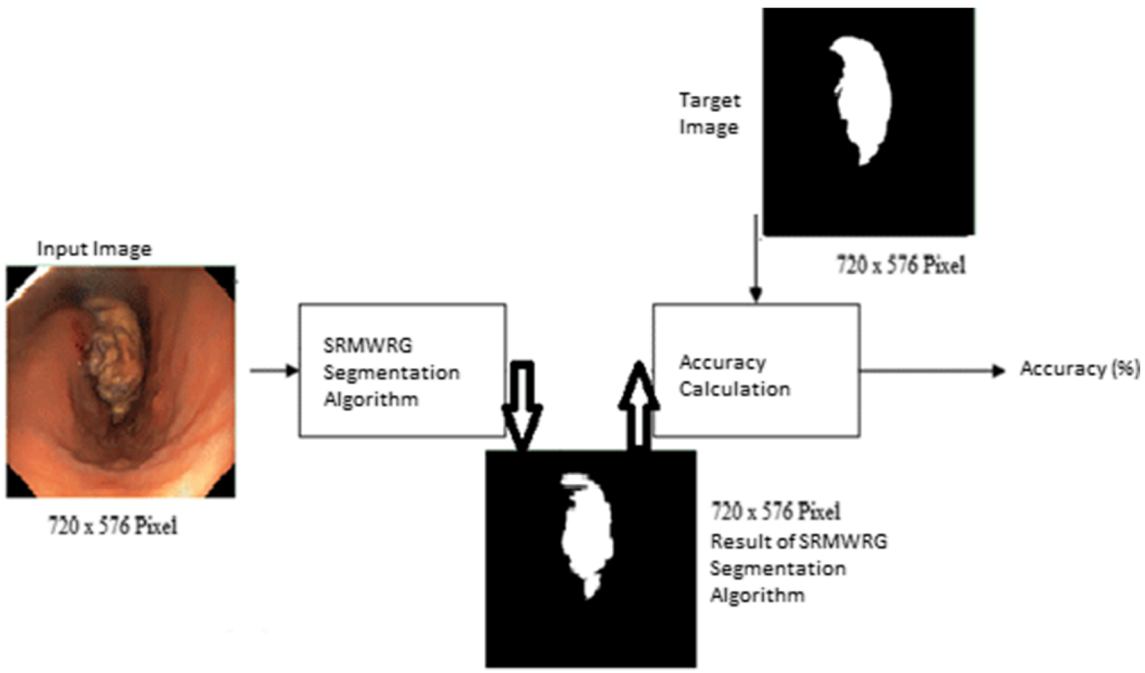

Fig. 10 Block schedules of the SRMWRG algorithm

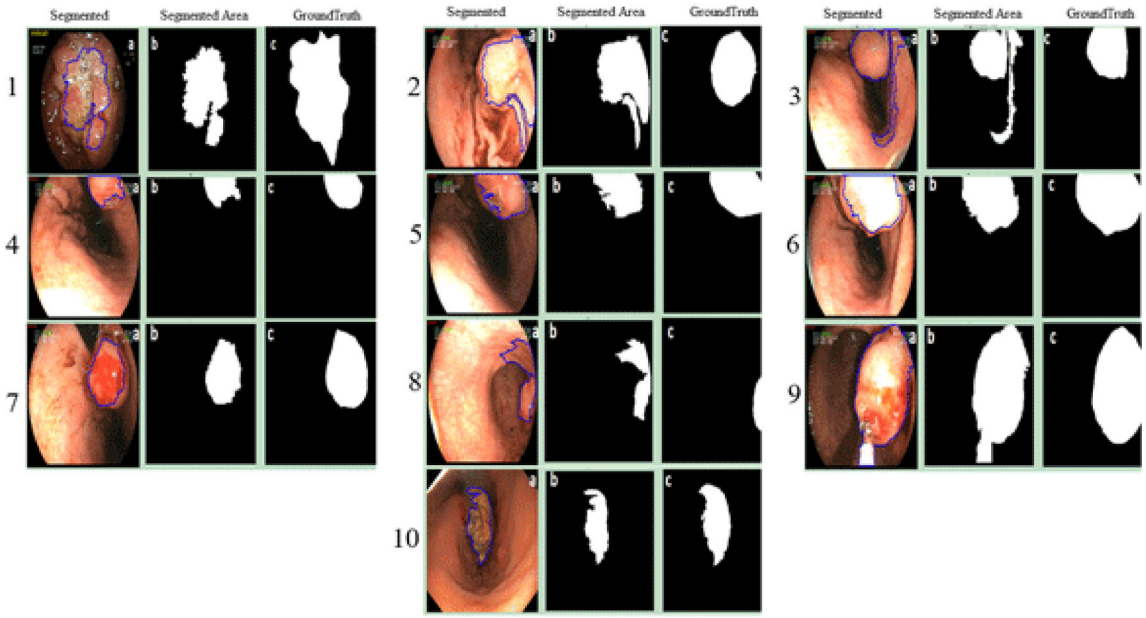

Fig. 11 Original Image, SRMWRG Segmented, Ground Truth Images

Table 3 shows the accuracy, sensitivity, specificity, ROC curve performance results and the average values of these SRMWRG segmented results.

Result and discussion

RG, SRM and SRMWRG were implemented to the endoscopy images of 10 different patients. In general the performance of such systems is evaluated using the data on the matrix. These data are shown on Table 4 [26]. There are several terms that are commonly used for the description of sensitivity, specificity and accuracy.

In conclusion, the Ground Truth images of the determined area are considered in evaluating the performance. The Ground Truth images are prepared with the help of a specialist doctor. In order to calculate these measurements, pixel by pixel matching of the output is made with the Ground Truth image. Sensitivity, specificity, recall, precision and accuracy are defined in terms of TP, TN, FN and FP. Classification performance without focusing on a class is the most general way of comparing algorithms. It does not favor any particular application. The introduction of a new learning problem inevitably concentrates on its domain but omits a detailed analysis. Therefore, the most used empirical measure, accuracy, does not distinguish between the numbers of correct labels of different classes [27]:

$$Accuracy = \frac{TP + TN}{TP + TN + FP + FN} \tag{6}$$

Table 3 TP, TN, FP, FN, Accuracy, Sensitivity, Specificity, Precision, ROC and F-Score Values

Application of Image Number	TN	TP	FP	FN	Accuracy	Sensitivity	Specificity	Precision	ROC Curve	F-Score
Image-1	282,520	78,510	1455	52,235	87,05	60,05	99,49	98,18	79,77	74,52
Image-2	309,482	50,347	39,261	15,630	86,76	76,31	88,74	56,19	82,53	64,72
Image-3	347,055	43,183	20,572	3910	94,10	91,70	94,40	67,73	93,05	77,91
Image-4	387,316	20,495	91	6818	98,33	75,04	99,98	99,56	87,51	85,58
Image-5	360,062	43,484	121	11,053	97,31	79,73	99,97	99,72	89,85	88,61
Image-6	330,051	66,670	0	17,999	95,66	78,74	100,00	100,00	89,37	88,11
Image-7	350,632	45,121	2	18,965	95,43	70,41	100,00	100,00	85,20	82,63
Image-8	376,539	13,857	16,671	7653	94,13	64,42	95,76	45,39	80,09	53,26
Image-9	268,677	120,669	20,532	4842	93,88	96,14	92,90	85,46	94,52	90,49
Image-10	372,308	33,470	6	8936	97,84	78,93	100,00	99,98	89,46	88,22
				Average (%)	94,05	77,15	97,12	85,22	87,13	79,40

Table 4 Terms used to define Accuracy, Sensitivity, Specificity, Precision, ROC and F-Score Values

Outcome of the diagnostic test	Condition (e.g. Disease) As Determined by the Standard of Truth		
	Positive	Negative	Row Total
Positive	TP	FP	TP + FP (Total number of subjects with positive test)
Negative	FN	TN	TN + FN (Total number of subjects with negative test)
Column Total	TP + FN (Total number of subjects with given condition)	FP + TN (Total number of subjects without given condition)	

Controversially, two measures that respectively estimate a classifier's performance on different classes are sensitivity and specificity (often employed in medical and biomedical applications, and in studies which cover image and visual data):

$$Sensitivity = \frac{TP}{TP + FN} = \text{Recall} \tag{7}$$

$$Specificity = \frac{TN}{TN + FP} \tag{8}$$

Focus on one class prevails in text classification, natural language processing, information extraction and bioinformatics, where the number of examples belonging to one class is frequently essentially lower than the whole number of examples. The experimental setting is as follows: within a set of classes there is a class of special interest (usually positive). Other classes are either left as is – multi-class classification – or combined into one – binary classification. The measures of selection calculated on the positive class are:

$$Precision = \frac{TP}{TP + FP} \tag{9}$$

F-score is a composite measure which favors algorithms with higher sensitivity and challenges those with higher specificity:

$$F{-}Score = 2{*}\frac{Precision{*}Sensitivity}{Precision + Sensitivity} \tag{10}$$

Table 5 Average results according to algorithms

Algorithms	Accuracy	Sensitivity	Specificity	Precision	ROC Curve	F-Score
RG	96,33	85,81	97,72	92,68	91,76	88,53
SRM	92,85	65,24	98,68	90,08	81,96	74,05
SRMWRG	94,05	77,15	97,12	85,22	87,13	79,40

The higher is the value of F-score, the better is the performance [28].

Accuracy, Sensitivity, Specificity, Precision, F-Score values are calculated as in Eqs. 6-10. Accuracy, Sensitivity, Specificity, Precision, ROC and F-Score values of 10 endoscopy images are given in Table 5 according to the algorithms used in our study.

Conclusion

In this study, endoscopy images obtained from patients who came to gastroenterology discipline were obtained from patients who were biopsied and diagnosed as pathologically proven cancer. Region growing (RG), Statistical Region Merging (SRM), Statistical Region Merging with Region Growing (SRMWRG) methods were applied to determine the cancerous area. The area obtained as a result of the applied methods should not be expressed as a definite cancerous region. However, this would prevent patients from being subjected to more endoscopy and biopsy by taking biopsy specimens from established areas instead of performing more than one biopsy procedure by specialist doctors. Thus, this study would have prevented the deterioration of patients' morale, the complications that may result in excessive biopsy, and the loss of faith that may arise against doctors.

As a result, it is seen that RG method produces more successful results, SRM method does not perform as well as RG, but SRMWRG method produces better results than SRM but it does not produce as good results as RG. Considering the hand-held values, we believe that gastric cancer will be helpful in determining the area and biopsy samples taken from the patient will be useful in determining the area. It is therefore considered a useful model.

Acknowledgements This work was supported by the project number 15101020 by Selcuk University Scientific Research Projects Coordination Office (BAP).

Compliance with Ethical Standards

Ethics Approval and Consent to Participate The whole study was approved by the local research ethics committee of Faculty of Medicine Affiliated to Selcuk University (Selçuklu, Konya Province, Turkey).

Conflicts of Interest The funders had no role in the design of the study; in the collection, analyses, or interpretation of data; in the writing of the manuscript, and in the decision to publish the results.

References

1. White, F. H., Gohari, K., and Smith, C. J., Histological and ultrastructural morphology of 7, 12 dimethyl Benz (alpha)-anthracene carcinogenesis in hamster cheek pouch epithelium. *Diagn. Histopathol.* 4(4):307–333, 1981.
2. Alpert, M. A., Terry, B. E., Mulekar, M., Cohen, M. V., Massey, C. V., Fan, T. M. et al., Cardiac morphology and left ventricular function in normotensive morbidly obese patients with and without congestive heart failure, and effect of weight loss. *Am. J. Cardiol.* 80(6):736–740, 1997.
3. Ural, B., Hardalaç, F., Serhatlioğlu, S., and İlhan, M. N., Gastric cancer regional detection system. *J. Med. Syst.* 40(1):31, 2016.
4. Brenner, H., Rothenbacher, D., and Arndt, V., Epidemiology of stomach cancer. *Cancer Epidemiol. Modifiable Factors*. 467–477, 2009.
5. Prof. Dr. K Yalçın POLAT https://www.memorial.com.tr/saglik-rehberleri/mide-kanseri/ "How to diagnose and treat stomach cancer", Last Access (03.08.2017).
6. Akbari, H., Kosugi, Y., Kojima, K., and Tanaka, N., Hyperspectral image segmentation and its application in abdominal surgery. *Int. J. Funct. Inf. Pers. Med.* 2(2):201–216, 2009.
7. Richardson, A. D., Duigan, S. P., and Berlyn, G. P., An evaluation of noninvasive methods to estimate foliar chlorophyll content. *New Phytol.* 153:185–194, 2002.
8. Dandıl, E., Ekşi, Z., & Çakıroğlu, M., Mamogram Görüntülerinden Bilgisayar Destekli Kitle Teşhisi Sistemi.
9. Jayas, D. S., and Karunakaran, C., Machine vision system in post-harvest tecnology. *Stewart Postharvest Rewiev.* 22, 2005.
10. Dalen, G. V., Determination of the size distribution and percentage of broken kernels of rice using flatbed scanning and image analysis. *Food Res. Int.* 37:51–58, 2004.
11. Neuman, M. R., Sapirstein, H. D., Shwedyk, E., and Bushuk, W., Wheat grain colour analysis by digital image processing. II. Wheat class discrimination. *J. Cereal Sci.* 10:183–188, 1989.
12. Karhan, M., Oktay, M. O., Karhan, Z., & Demir, H.,. Morfolojik görüntü işleme yöntemleri ile kayısılarda yaprak delen (çil) hastalığı sonucu oluşan lekelerin tespiti. In 6th International Advanced Technologies Symposium (IATS'11) (pp 172–176), 2011.
13. Keefe, P. D., A dedicated wheat grain image analyzer. *Plant Varieties Seeds* 5:27–33, 1992.
14. Mookiah, M. R. K., Rajendra Acharya, U., Martis, R. J., Chua, C. K., Lim, C. M., Ng, E. Y. K., and Laude, A., Evolutionary algorithm based classifier parameter tuning for automatic diabetic retinopathy grading: A hybrid feature extraction approach. *Knowl.-Based Syst.* 39:9–22, 2013.
15. Pratta, H., Coenenb, F., Broadbentc, D.M., Hardinga, S.P., and Zhenga, Y., Convolutional neural networks for diabetic retinopathy. *Procedia Comp Sci*. 200–205, 2016.
16. Camps-Valls, G., and Bruzzone, L., Kernel-based methods for hyperspectral image classification. *IEEE Trans. Geosci. Remote Sens.* 43:1351–1362, 2005.
17. Moran, J. A., Mitchell, A. K., Goodmanson, G., and Stockburger, K. A., Differentiation among effects of nitrogen fertilization treatments on conifer seedlings by foliar reflectance: A comparison of methods. *Tree Physiol.* 20:1113–1120, 2000.
18. Xuan, J., Adali, T., and Wang, Y., Segmentation of magnetic resonance brain image: integrating region growing and edge detection. Image Processing, 1995. Proceedings, International Conference on. Vol. 3. IEEE, 1995.
19. Ballard, D.H., Brown C.M., Computer Vision (pp 149), 1982.
20. Tang, J., A color image segmentation algorithm based on region growing. In Computer engineering and technology (iccet), 2010 2nd international conference on (Vol. 6, pp. V6-634). IEEE., (2010, April).
21. Yasar, A., Saritas, I., Korkmaz, H., The detection of stomach cancer with semi-automatic region growing segmentation method. Ciencia e Tecnica Vitivinicola Journal (ISSN: 0254-0223), 206–220, 2017.
22. Gonzalez, R. C., Woods, R. E., Digital image processing. Singapore: Pearson Education, 2014.
23. Subudhi, B. N., Thangaraj, V., Sankaralingam, E., and Ghosh, A., Tumor or abnormality identification from magnetic resonance images using statistical region fusion based segmentation. *Magn. Reson. Imaging* 34(9):1292–1304, 2016.
24. Celebi, M. E., Kingravi, H. A., Iyatomi, H., Lee, J., Aslandogan, Y. A., Van Stoecker, W., ... & Marghoob, A. A., Fast and accurate border detection in dermoscopy images using statistical region merging. SPIE., (2007, March).
25. Li, H., Gu, H., Han, Y., and Yang, J., An efficient multiscale SRMMHR (statistical region merging and minimum heterogeneity rule) segmentation method for high-resolution remote sensing imagery. *IEEE J. Sel. Top. Appl. Earth Observ. Remote Sens.* 2(2):67–73, 2009.
26. Zhu, W., Zeng, N., and Wang, N., Sensitivity, specificity, accuracy, associated confidence interval and ROC analysis with practical SAS implementations. NESUG proceedings: health care and life sciences, Baltimore, Maryland, 19, 2010.
27. Sokolova, M., Japkowicz, N., and Szpakowicz, S., Beyond accuracy, F-score and ROC: a family of discriminant measures for performance evaluation. In Australasian joint conference on artificial intelligence (pp 1015–1021). Springer, Berlin, Heidelberg, (2006, December).
28. Toulouse, T., Rossi, L., Celik, T., and Akhloufi, M., Automatic fire pixel detection using image processing: A comparative analysis of rule-based and machine learning-based methods. *SIViP.* 10(4):647–654, 2016.